

Chapter 4

Dielectric Relaxation in Polymeric Materials

4.1. Introduction

Over this last decade, the technological development of dielectric spectroscopy on the one hand [MCC 67], [BLY 79], [KRE 02], and dielectric thermal analysis on the other [VAN 75], [HED 77], [RUN 97], have allowed the development of dielectric relaxation studies in a wide frequency (from 10^{-6} to 10^{+11} Hz) and temperature range, thus leading to a new approach of behavior laws of dielectric relaxation in polymeric materials. In the same way, the development of physico-chemistry and polymer physics [CAR 99], [FON 02], [RAU 02], [HAL 06], [PER 92], [STR 97] has improved the interpretation of the mechanisms observed at a molecular scale.

4.2. Dynamics of polarization mechanisms

The polarization mechanisms are of different origins: (1) from the modification of spatial distributions of electronic and ionic elementary particles and (2) from the reorientation of dipolar entities. These mechanisms are multi-scale and the kinetics to establish the polarization exists at very different time and frequency ranges. We are going to cite them in order of increasing establishment time.

4.2.1. Electronic and ionic polarization

Under the influence of an external electric field, the electronic orbits are distorted with very fast kinetics (10^{-15} s) causing electronic polarization (see Figure 4.1). The ionic displacements will be made with slower kinetics (10^{-13} s): they are responsible for the ionic polarization (see Figure 4.1).

Considering the establishment time of all of these mechanisms, they behave as instantaneous phenomena in the time domain, and are observed at much higher frequencies than those of electric fields used in dynamical dielectric spectroscopy. This polarization will be designated by P_∞ and is related to the permittivity at infinite frequency ϵ_∞ by the equation:

$$P_\infty = (\epsilon_\infty - 1)\epsilon_0 E \quad [4.1]$$

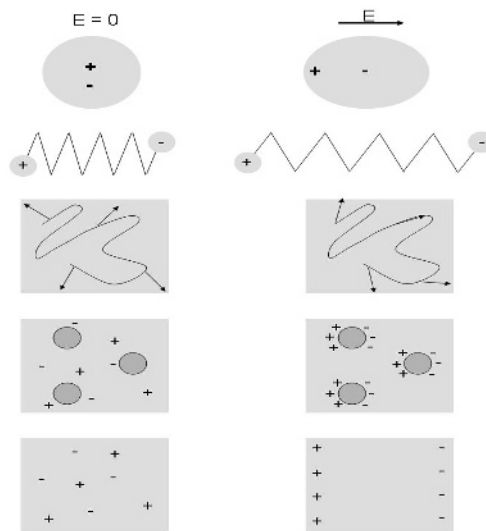


Figure 4.1. Schematic representation of polarization mechanisms.
From top to bottom: electronic, ionic, dipolar,
Maxwell–Wagner–Sillars, and inter-facial polarizations

4.2.2. Dipolar polarization

Polymeric materials are made of more or less polar entities, of different (sub- or super-nanometric) scales. Their reorientation, which tends to align them in the direction of the electric field, is the cause of the dipolar orientation polarization P_d .

The time/frequency scale is now of the order of that covered by dielectric spectrometries. This dipolar polarization P_d is associated with the permittivity ϵ_d by the relation:

$$P_d = \epsilon_d \epsilon_0 E \quad [4.2]$$

P_s is the total acquired polarization, in established regime:

$$P_s = (\epsilon_s - 1) \epsilon_0 E \quad [4.3]$$

where ϵ_s is the static permittivity.

The variation amplitude of the dipolar polarization is then:

$$P_s - P_\infty = (\epsilon_s - \epsilon_\infty) \epsilon_0 E \quad [4.4]$$

4.2.3. Maxwell–Wagner–Sillars polarization

Any heterogeneity of the dielectric can lead to the accumulation of charges at the interfaces if the structural entities (amorphous and crystalline phases in the semi-crystalline polymers) or morphological (polymer matrix and reinforcement in the composites) have different conductivities (see Figure 4.1). It is then made of relaxing entities likely to turn towards long/low frequency times.

4.2.4. Interfacial polarization

The charges trapped on the surface of the sample make a macro dipole whose characteristic dimension corresponds to the thickness of the sample (see Figure 4.1). For small thicknesses, the relaxation of this macro dipole takes place at very long/very low frequency times, with a very strong intensity. Like the Maxwell–Wagner–Sillars polarization, the inter-facial polarization is distinguished from the orientation polarization by a much stronger intensity.

4.3. Orientation polarization in the time domain

To have a simple qualitative description of the establishment of the orientation polarization, the hypothesis of first order kinetics is widely used. After recalling the basic equation of this analogical modeling, the principal analytical equations will allow a quantitative description of the experimental results [BOT 78].

4.3.1. Single relaxation time model

τ is the relaxation time characteristic of the polarization kinetics establishment. The dipolar polarization is defined by the first order differential equation:

$$\tau \frac{dP_d(t)}{dt} + P_d(t) = (\varepsilon_s - \varepsilon_\infty) \varepsilon_0 E \quad [4.5]$$

Under static field $E = E_0$, considering the boundary conditions on P_d , the solution is written:

$$P_d = (\varepsilon_s - \varepsilon_\infty) \varepsilon_0 E \left(1 - \exp\left(-\frac{t}{\tau}\right) \right) \quad [4.6]$$

In this model, the dielectric permittivity is given by:

$$\varepsilon(t) = \varepsilon_\infty + (\varepsilon_s - \varepsilon_\infty) \left(1 - \exp\left(-\frac{t}{\tau}\right) \right) \quad [4.7]$$

This variation is generally represented as a function of $\log t$. It is a sigmoid which presents no element of symmetry. The description of the experimental results is correct qualitatively and not quantitatively.

4.3.2. Discrete distribution of relaxation times

The dielectric polymers are heterogenous, at different scales, both nanometric and micronic. To refine the description of experimental results, a discrete distribution of relaxation time (τ_j) with a dispersion ($\varepsilon_s - \varepsilon_\infty$)_{*j*} represents an interesting approach. The dielectric permittivity is then written:

$$\varepsilon(t) = \varepsilon_\infty + \sum_j (\varepsilon_s - \varepsilon_\infty)_j \left(1 - \exp\left(-\frac{t}{\tau_j}\right) \right) \quad [4.8]$$

– with: $\sum_j (\varepsilon_s - \varepsilon_\infty)_j = (\varepsilon_s - \varepsilon_\infty)$

4.3.3. Continuous distribution of relaxation times

If an homogenization of the medium at a certain scale is realistic, the use of a continuous distribution function $\phi(\ln\tau)$ is relevant; it allows us to work with global responses. The dielectric permittivity is given by:

$$\varepsilon(t) = \varepsilon_{\infty} + (\varepsilon_s - \varepsilon_{\infty}) \int_0^{\infty} \phi(\ln\tau) \left(1 - \exp\left(-\frac{t}{\tau}\right)\right) d \ln \tau \quad [4.9]$$

with: $\int_0^{\infty} \phi(\ln\tau) d \ln \tau = 1$

4.3.4. Stretched exponential: Kohlrausch–Williams–Watts equation

In the same way as the homogenous medium, the use of the stretched exponential is interesting because it is analytically simpler:

$$\varepsilon(t) = \varepsilon_{\infty} + (\varepsilon_s - \varepsilon_{\infty}) \left\{ 1 - \exp\left(-\left(\frac{t}{\tau}\right)^{\beta_{KWW}}\right) \right\} \quad [4.10]$$

with: $0 < \beta_{KWW} \leq 1$

4.4. Orientation polarization in the frequency domain

The description of the dynamic orientation polarization is made with the same methodology as for the transitory polarization since they are related by the Laplace transformation.

4.4.1. Single relaxation time model: the Debye equation

In the presence of a dynamic electric field $E = E_0 \cos \omega t$, represented by the complex expression $E^* = E_0 \exp(i\omega t)$, the solution, in an established regime, of differential equation [4.5] is:

$$\varepsilon_d^*(\omega) = \frac{(\varepsilon_s - \varepsilon_{\infty})}{(1 + i\omega\tau)} \quad [4.11]$$

The total complex permittivity:

$$\varepsilon^*(\omega) \equiv \varepsilon'(\omega) - i\varepsilon''(\omega) \quad [4.12]$$

is then defined by:

$$\varepsilon'(\omega) = \varepsilon_\infty + (\varepsilon_s - \varepsilon_\infty) \times \frac{1}{1 + \omega^2\tau^2} \quad [4.13]$$

$$\varepsilon''(\omega) = (\varepsilon_s - \varepsilon_\infty) \times \frac{\omega\tau}{1 + \omega^2\tau^2} \quad [4.14]$$

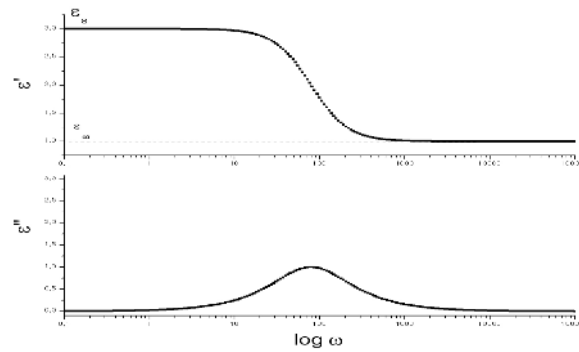


Figure 4.2. Complex permittivity predicted by the Debye equation:
 $\varepsilon'(\log\omega)$ and $\varepsilon''(\log\omega)$

These expressions are designated in the literature by the Debye equations. The variation laws of ε' and ε'' as a function of $\log \omega$ are represented in Figure 4.2. They present elements of symmetry which are not observed in the experimental variations.

4.4.2. Discrete distribution of relaxation times

For heterogenous materials, the complex permittivity is well described by:

$$\varepsilon^*(\omega) \equiv \varepsilon_\infty + \sum_j \frac{(\varepsilon_s - \varepsilon_\infty)_j}{(1 + i\omega\tau_j)} \quad [4.15]$$

By using fractional polarizations, the analysis of thermo-stimulated currents allows the parameters $(\epsilon_s - \epsilon_\infty)_j$ and τ_j to be accessed.

4.4.3. Continuous distribution of relaxation times

For homogenous materials, the approach using a continuous distribution of relaxation times is interesting:

$$\epsilon^*(\omega) = \epsilon_\infty + (\epsilon_s - \epsilon_\infty) \int_0^\infty \frac{\varphi(\ln \tau)}{1 + i\omega\tau} d \ln \tau \quad [4.16]$$

4.4.4. Parametric analytical expressions

To describe the experimental results, numerous parametric expressions have been proposed [JON 83]. To take a didactic approach, we shall only cite those resulting in the Havriliak and Negami equation, which is currently the most widely used.

4.4.4.1. Cole–Cole equation

The equation proposed by Cole–Cole allows a widening of the relaxation zone and thus permits a better description of the experimental results.

$$\epsilon^*(\omega) = \epsilon_\infty + \frac{(\epsilon_s - \epsilon_\infty)}{1 + (i\omega\tau)^{\beta_{CC}}} \quad [4.17]$$

with: $0 < \beta_{CC} \leq 1$

4.4.4.2. Havriliak and Negami equation

The experimental results show an asymmetry of the variation law which is not taken into account by equation [4.17]. The Havriliak and Negami equation allows the description to be optimized by the introduction of an additional parameter [HAV 67], [HAV 97]:

$$\epsilon^*(\omega) = \epsilon_\infty + \frac{(\epsilon_s - \epsilon_\infty)}{\left(1 + (i\omega\tau)^{\beta_{HN}}\right)^{\gamma_{HN}}} \quad [4.18]$$

with: $0 < \beta_{HN} \leq 1$ and $0 < \gamma_{HN} \leq 1$

4.4.4.3. Cole–Cole representation

By eliminating the frequency between the two Debye equations, [4.13] and [4.14], a relation between ϵ' and ϵ'' is obtained. It can be written as [COL 41]:

$$\left\{ \epsilon' - \frac{\epsilon_s + \epsilon_\infty}{2} \right\}^2 + \epsilon''^2 = \left\{ \frac{\epsilon_s - \epsilon_\infty}{2} \right\}^2 \quad [4.19]$$

This variation law which corresponds to the model of a single relaxation time is represented in the complex plan in Figure 4.3. We have also reported, for comparison, the variation law ϵ'' (ϵ') corresponding to the Havriliak and Negami equation with the parameters $\beta_{HN} = 0.6$ and $\gamma_{HN} = 0.4$. The advantage of this representation is to give an estimation of the parameters from the geometric construction.

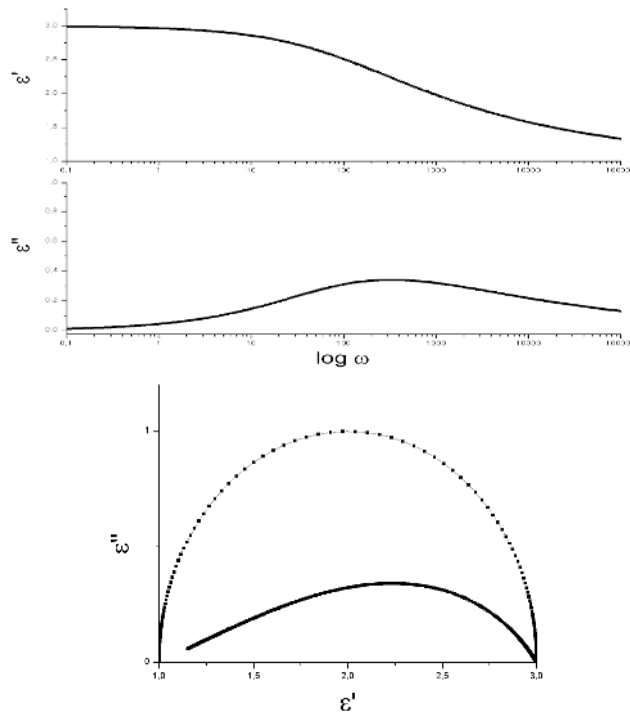


Figure 4.3. Complex permittivity predicted by the Havriliak and Negami equation with $\beta_{HN} = 0.6$ and $\gamma_{HN} = 0.4$: ϵ' ($\log \omega$); ϵ'' ($\log \omega$); ϵ'' (ϵ') in the continuous line – the dotted line corresponds to the Debye equation

4.4.5. *Kramers–Kronig relations*

ε' and ε'' are related by the Kramers–Kronig relationships:

$$\varepsilon'(\omega) - \varepsilon_\infty = \left(\frac{2}{\pi}\right) \int_0^\infty \frac{u \varepsilon''(u)}{u^2 - \omega^2} du \quad [4.20]$$

$$\varepsilon''(\omega) = \left(\frac{2}{\pi}\right) \int_0^\infty \frac{\varepsilon'(u) - \varepsilon_\infty}{u^2 - \omega^2} du \quad [4.21]$$

These equations were first used in the optical frequency domain. For dielectric relaxation, they are very useful to identify the dielectric energy loss of dipolar origin which can be hidden by electrical conduction.

4.5. Temperature dependence

The temperature dependence of the relaxation time is always exponential; the variation and dispersion ($\varepsilon_s - \varepsilon_\infty$) is a powerful law. For a first approximation, we shall uniquely consider the temperature variation of the relaxation time.

4.5.1. *Shift factor*

In this approximation, temperature causes a simple translation of spectra along the axis $\log t / \log \omega$. The shift factor a_T defines this geometric operation which transforms the isotherm T_0 into isotherm T [FER 70].

4.5.1.1. *Time domain*

The shift factor will be designed by a_{Tt} in the time domain. This is:

$$\log a_{Tt} = \frac{\log \tau(T)}{\log \tau(T_0)} \quad [4.22]$$

4.5.1.2. *Frequency domain*

The shift factor will be designated by $a_{T\omega}$ in the frequency domain. We can easily verify that:

$$\log a_{Tt} = -\log a_{T\omega} \quad [4.23]$$

4.5.2. Crystalline or vitreous phases: Arrhenius equation

For the crystalline or vitreous phases, the temperature dependence of the relaxation time has the same phenomenological behavior. It can be described by the barrier theories already used by Fröhlich [FRO 58] to describe the dielectric relaxation in the crystals. They have been adjusted to molecular crystals by Hoffman [MCC 67].

4.5.2.1. Thermal activation mechanism

In the barrier theories, the environment of the relaxing entity is represented by the variation of the Gibbs free enthalpy G . The orientation of the relaxing entities corresponds to the crossing of energetic barriers separating the different minima of G , by thermal activation. A classical description by Boltzmann equations gives, for the transition probability p , a variation as:

$$p \propto \exp \frac{-\Delta G}{RT} \quad [4.24]$$

where ΔG represents the height of the enthalpic barrier which separates the two sites and R the ideal gas constant.

The relaxation time, which varies in the opposite direction to the probability, is in the form:

$$\tau = \tau_0 \exp \frac{\Delta G}{RT} \quad [4.25]$$

To obtain an explicit equation as a function of temperature, we must express ΔG as a function of the activation enthalpy ΔH and of the activation entropy ΔS :

$$\tau = \tau_0 \exp - \frac{\Delta S}{R} \exp \frac{\Delta H}{RT} \quad [4.26]$$

$$\text{So: } \tau_{0a} = \tau_0 \exp - \frac{\Delta S}{R}$$

$$\tau = \tau_{0a} \exp \frac{\Delta H}{RT} \quad [4.27]$$

This is the Arrhenius equation. The corresponding variation of $\log \tau$ as a function of T^{-1} is represented in Figure 4.4.

4.5.2.2. Interpretation of the activation parameters

The activation enthalpy is directly related to the cohesion of the phase in which the relaxation is done: in a crystalline phase it will be higher than in a vitreous phase. It also depends on the size of the relaxing entity. The activation entropy comes from the Boltzmann equation:

$$\Delta S = R \ln \Omega \quad [4.28]$$

if Ω is the number of sites accessible to the relaxing entity. τ_0 can be deduced from Eyring's chemical activation theory [EYR 36]:

$$\tau_0 = \frac{h}{kT} \quad [4.29]$$

In the crystalline phases, Ω is near unity; τ_{0a} will then be of the order of time constants associated with infrared frequencies. In the vitreous phases, Ω is very high so τ_{0a} very low. This permits the observed relaxation phenomena in semi-crystalline polymers to be localized in one or other of these phases.

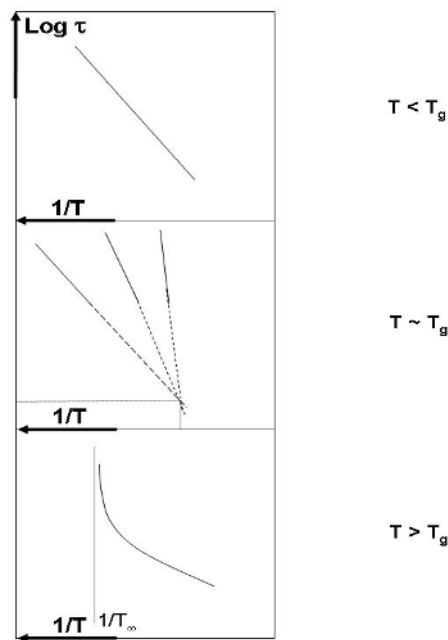


Figure 4.4. Temperature dependence of relaxation times in the three indicated temperature zones

4.5.3. *Vitreous phases in the transition zone: the Hoffman–Williams–Passaglia equation*

To describe the dielectric relaxations in a series of paraffins with different lengths, Hoffman–Williams–Passaglia (HWP) [HOF 66] have made the following hypothesis: the activation enthalpies ΔH_j and the activation entropies ΔS_j of the paraffin composed of j constitutive units are linear functions of the activation enthalpies ΔH_0 and entropies ΔS_0 for each constitutive unit. ΔH_j and ΔS_j are therefore expressed by:

$$\Delta H_j = j\Delta H_0 + \Delta H_1 \quad [4.30]$$

$$\Delta S_j = j\Delta S_0 + \Delta S_1 \quad [4.31]$$

ΔH_1 and ΔS_1 represent the activation enthalpies and entropies of the chain extremities. ΔH_j is therefore a linear function of ΔS_j .

with $T_c \equiv \Delta H_0/\Delta S_0$, equation [4.2] is now written:

$$\tau_j = \tau_c \exp\left\{\frac{\Delta H_j}{R}(T^{-1} - T_c^{-1})\right\} \quad [4.32]$$

where the constant τ_c represents the relaxation time at temperature T_c . This “compensation law” which has been established for the relaxation times of paraffins made up of j constitutive units, also describes the different relaxation times isolated in a polymer in the vitreous transition zone. In this case, they reflect the relaxation of entities with different lengths of polymer chain sequences. The behavior of these relaxation times is represented in Figure 4.4.

4.5.4. *Liquid phases: Vogel–Fulcher–Tammann equation (VFT)*

For liquid phases, the dielectric relaxation time has the same temperature dependence as the viscosity. It is described by the free volume theories proposed by Cohen Turnbull [COH 59] for inorganic amorphous materials as well as by the thermodynamic theory of Adam and Gibbs [ADA 65]. We shall content ourselves here with presenting the free volume concept.

4.5.4.1. Free volume concept

The specific volume v_s of a polymer is composed of two terms:

- the volume occupied by the constitutive groups of the macromolecule v_o , due to steric hindrance and thermal agitation; and
- the free volume v_f

The basic hypothesis of volume theories is the following: the molecular mobility is liberated when the free volume is greater than a critical value v^* . The relaxation time is then dependent on the fraction of free volume $f \equiv v_f / v^*$. From the free volume theory, we obtain:

$$\tau = \tau_{0V} \exp\left(\frac{1}{f}\right) \quad [4.33]$$

where τ_{0V} is independent of the temperature.

To explain the dependence on temperature, another hypothesis is necessary; above the critical temperature T_∞ , the fraction of free volume is expanded according to the relation:

$$f = \alpha_f (T - T_\infty) \quad [4.34]$$

where α_f represents the expansion coefficient of the free volume fraction.

The explicit equation of the relaxation time is then:

$$\tau = \tau_{0V} \exp\left\{\frac{1}{\alpha_f (T - T_\infty)}\right\} \quad [4.35]$$

Figure 4.4 shows this variation law on an Arrhenius diagram. This equation has been widely used in the literature [VOG 21], [FUL 52], [TAM 26] and is known by as the Vogel–Fulcher–Tammann equation. Let us note that T_∞ is then the temperature under which the molecular mobility is fixed. In the thermodynamic theory of Gibbs and Di Marzio, it is the temperature at which the activation entropy is null. Analytically, it is defined as the temperature T_∞ which linearizes the variation of $\ln \tau$ as a function of $1/(T - T_\infty)$.

4.5.4.2. Williams–Landel–Ferry empirical expression (WLF)

The shift factor has been widely used in this temperature zone to describe molecular mobility, in particular by Williams–Landel–Ferry [FER 70] who have proposed an empirical equation:

$$\log a_{T_i} = -\frac{c_{10}(T - T_0)}{(c_{20} + T - T_0)} \quad [4.36]$$

c_{10} is a dimensionless constant; c_{20} has the same dimension as temperature. Considering the definition of the displacement factor (see equation [4.23]), this empirical equation is equivalent to the Vogel–Fulcher–Tammann equation. For amorphous polymers having a vitreous transition temperature of less than 100°C, for a reference temperature $T_0 = T_g$, universal values are obtained for both constants: $c_{1g} = 17.44$ and $c_{2g} = 51.6^\circ$. The corresponding values of the VFT equation are $a_f = 4.84 \cdot 10^{-4} (\text{°})^{-1}$ and $T_\infty = T_g - 51.6^\circ$.

4.6. Relaxation modes of amorphous polymers

The dielectric relaxations associated with the dipolar reorientation reflect the different organization levels of the polymer. We shall consider them in the order of increasing frequencies on an isochronous spectrum: the primary relaxation mode, thus designated because generally the most intense, is often called relaxation α ; the secondary relaxation modes are multiple (β , γ , δ). To simplify, we shall adopt the same nomenclature for amorphous and semi-crystalline polymers, which is not necessarily the case in the literature. The monophasic amorphous polymers present the simplest relaxation spectra.

4.6.1. Primary relaxation mode

4.6.1.1. Complex relaxation in an homogenous liquid medium

When it is observed after the vitreous transition, this relaxation mode can be treated like a complex relaxational event in an homogenous medium. As shown in the example in Figure 4.5 for an amorphous PET [MEN 99], the Havriliak and Negami equation allows the variation of the dissipative component of the permittivity $\epsilon''(\log\omega)$ to be described correctly.

The relaxation time τ_{HN} obeys a VFT equation with a critical temperature of $T_g - 40^\circ\text{C}$, not very far from WLF values. This result is coherent with the fact that, considering the frequency range covered in dielectric spectrometry; this relaxation mode is observed in the liquid state. This temperature behavior of the relaxation time is typical of “weak” liquids [ANG 95] i.e. those whose cohesion in the amorphous phase implies weak physical bonding. In the opposite case, the relaxation time obeys an Arrhenius equation: the poly(methyl methacrylate) PMMA has the typical behavior of “strong” liquids.

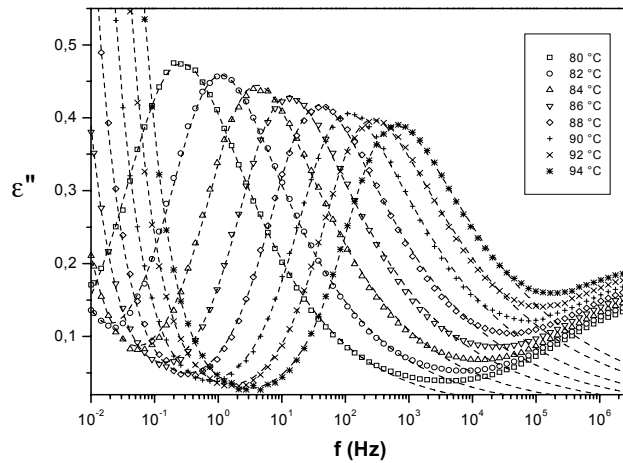


Figure 4.5. Isothermal dynamic spectra of dielectric loss: the primary relaxation mode of an amorphous polymer (PET)

4.6.1.2. Discrete spectrum of simple relaxations in a heterogenous vitreous medium

This mode has also been studied in thermo-stimulated currents: by the weak equivalent frequency of this technique (10^{-2} Hz), the relaxation is then produced in the vitreous state. This mode can then be resolved by fractional polarizations, in a discrete series of elementary relaxational phenomena represented in Figure 4.6; the activation parameters of each one are reported in Figure 4.7.

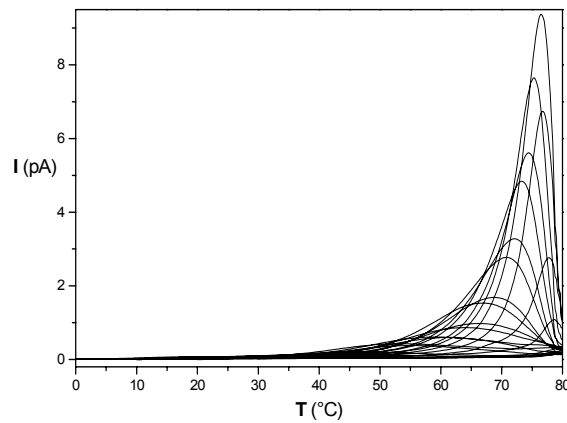


Figure 4.6. Elementary thermograms of thermo-stimulated current for a primary relaxation mode: example of an amorphous polymer (PET)

The observation of a compensation law (equation [4.32]) indicates the cooperativity of this molecular mobility. It is important to note that the compensation temperature is of the order of the vitreous transition temperature, and the compensation time τ_c is about 10 seconds, i.e. the time constant values associated with the vitreous transition. By analogy with the Hoffmann–Williams–Passaglia model, the elementary mechanisms have been associated with the mobility of chain sequences (of the order of nanometres) with different lengths which are liberated by the gradual rupture of the physical bonding in the vitreous transition mechanism.

It is important to note the universality of this behavior, independently of the structure and, in particular, the architecture of the polymer chain. Moreover, the activation parameter values reflect the cohesion of the amorphous phase.

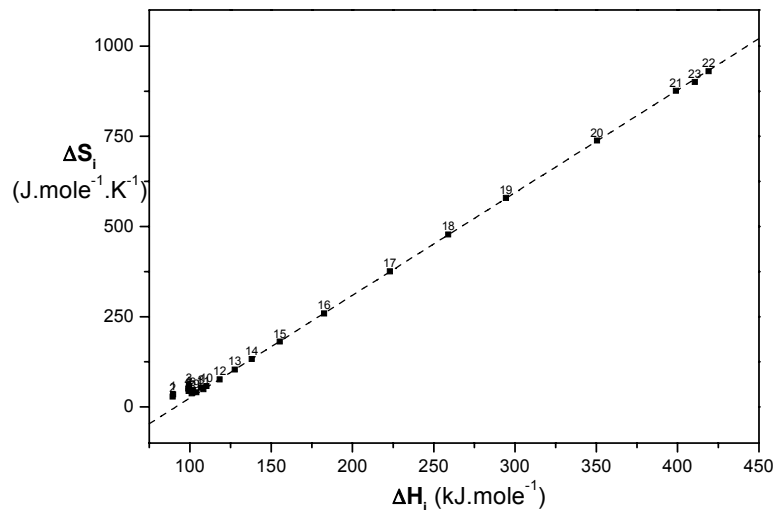


Figure 4.7. Compensation diagram deduced from analysis of thermo-stimulated current for an amorphous polymer (PET)

4.6.2. Secondary relaxation modes

4.6.2.1. Specific mobility of the chemical structure

The polymers which have a polar lateral chain present a relaxation mode specific to this lateral chain. As the dielectric surface of the atactic PMMA reported in Figure 4.8 shows, it is sometimes more intense than the primary relaxation. This is produced in the vitreous phase and is then associated with a localized mobility.

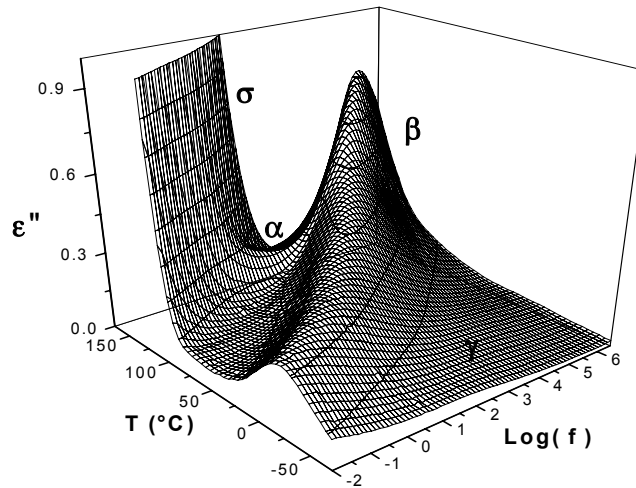


Figure 4.8. Dielectric surface deduced from dynamic spectroscopy for an amorphous polymer with lateral chain (PMMA)

4.6.2.2. Mobility of the main chain

The vitreous phase presents a localized molecular mobility of the main chain responsible for a generic secondary relaxation, which is illustrated in Figure 4.9 by the isochrone $\epsilon''(T)$ recorded for an amorphous PET. This is a mobility of sub-micronic sequences which is the cause of this relaxation mode.

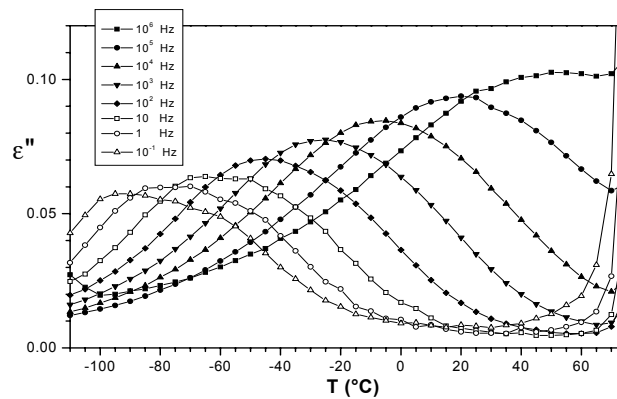


Figure 4.9. Isochronous dynamic spectroscopy of the secondary relaxation of an amorphous polymer (PET)

4.7. Relaxation modes of semi-crystalline polymers

In general, semi-crystalline polymers present a primary relaxation which is the most intense, as shown by the dielectric surface of the PVDF represented in Figure 4.10 [MEN 99].

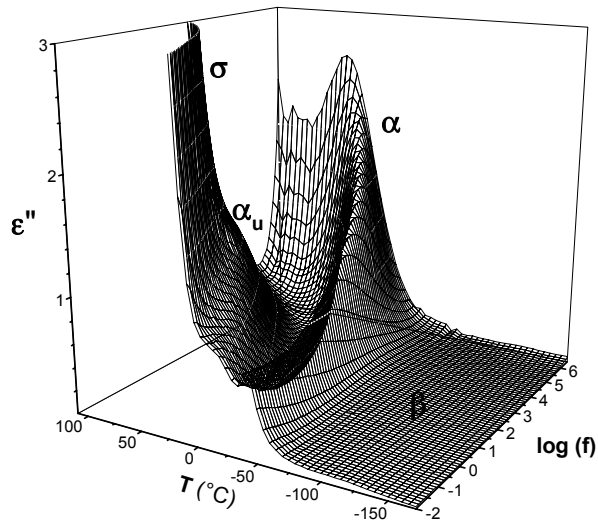


Figure 4.10. Dielectric surface deduced from dynamic spectroscopy for a semi-crystalline polymer (PVDF)

These results were obtained from dielectric spectroscopy. The increase of energy losses towards high temperatures is explained by the existence of a significant electrical conduction brought to the fore because the measurements are taken under an electric field. As for amorphous polymers, a secondary relaxation β is observed. In the zone where the amorphous phase is liquid, an additional relaxation α_u is produced.

The shift kinetics of the different relaxation modes is reported in Figure 4.11. To illustrate relaxation kinetics characteristic of a polymer, the figure shows the Arrhenius diagram of the relaxation times for the PVDF. The experimental points corresponding to the relaxation times shorter than 10 seconds come from measurements in dielectric spectrometry; those corresponding to the relaxation times longer than 10 seconds come from measurements in TSC. The elementary processes are spotted by indices, in order of increasing temperatures, as in Figure 4.12.

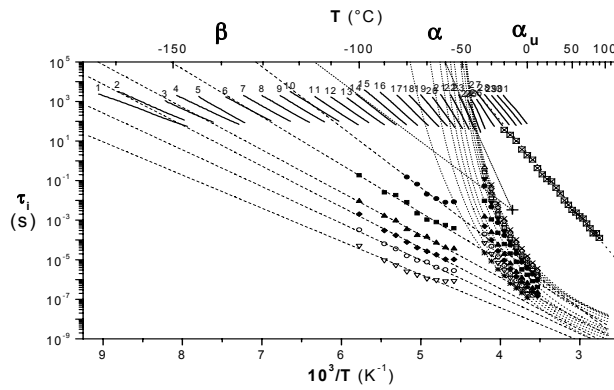


Figure 4.11. Arrhenius diagram of the relaxation times for a semi-crystalline polymer (PVDF)

4.7.1. Complex relaxation in an homogenous medium

For the relaxation mode β , the constitutive processes always behave in a way which obeys an Arrhenius equation: this molecular mobility localized at the sub-micronic scale is thermally activated in semi-crystalline polymers, as in amorphous polymers.

4.7.2. Discrete spectrum of elementary relaxations in a heterogenous medium

The results of the TSC analysis, in terms of the discrete distribution of relaxation time, for the PVDF are reported on a compensation diagram (see Figure 4.12).

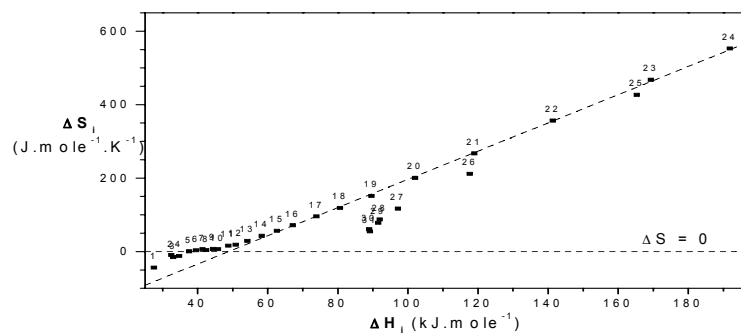


Figure 4.12. Compensation diagram deduced from analysis of thermo-stimulated current for a semi-crystalline polymer (PVDF)

Three types of behaviors appear. For the processes of weaker enthalpy, the activation entropy remains practically null. Following Starkweather's nomenclature [STA 83], these constitutive processes of the β mode are due to a non-cooperative localized molecular mobility. The processes which follow the compensation law with linearly dependent enthalpy/entropy activation parameters correspond to the cooperative molecular mobility liberated at the vitreous transition. They correspond to the primary relaxation. The processes which are characterized by activation parameters of the same order have been localized in the para crystalline phase: the processes are initiated by the conformational defects.

4.7.3. Universality of the behavior laws in semi-crystalline polymers

In semi-crystalline polymers, the molecular motions can be made either in the amorphous phase, or in the crystalline phase. From this fact, the relaxation modes are in general more complex than in amorphous polymers. This complexity affects, in particular, the secondary relaxation modes. Thus the β mode of the amorphous PET cleaves into two components in the semi-crystalline PET [MEN 99]. Whatever the localization of secondary relaxations, the constitutive processes are always thermally activated with energetic barriers of less than 50 kJoules/mole.

The primary relaxation has the same phenomenological behavior in semi-crystalline polymers as in amorphous polymers. It is obviously very sensitive to physical ageing [STR 75]. For "weak" liquid polymers, like the PVDF, a discontinuity of the behavior law is observed with cooperative thermally activated processes below T_g and a complex mode governed by the free volume above T_g . For semi-crystalline polymers with "strong" liquid-like polyamids, the behavior above T_g remains thermally activated.

Complementary relaxation modes are observed above T_g in most semi-crystalline polymers. For polymers with a semi-rigid chain whose crystallization kinetic is slow, like the PET and the PEEK, the primary relaxation mode has an additional high temperature component around $T_g + 20^\circ\text{C}$. It corresponds to a thermally activated molecular mobility of the "rigid" amorphous phase [BOT 75]. For polymers with a flexible chain like the PVDF or the PEBD, it is the thermally activated molecular mobility of the para-crystalline zones which is observed above vitreous transition.

4.8. Conclusion

In polymeric materials, the localized molecular mobility at the origin of the secondary relaxations is obviously conditioned by the chemical structure

(polar/apolar, flexible/rigid, etc.) of the constitutive unit. The delocalized molecular mobility at the origin of the primary relaxation is directly related to the evolution of the physical structure (glass/liquid) and has, therefore, a kinetic character. To control this phenomenon, we have to take into account the thermodynamic history of this material. As for the structural heterogeneities, they obviously have an essential role at low frequency. In the future, studies will allow dielectric relaxations in polymeric materials to be predicted and controlled.

4.9. Bibliography

- [ADA 65] ADAM G., GIBBS J.H., *J. Chem. Phys.*, 43, 1, p. 139, 1965.
- [ANG 95] ANGELL C.A., *Science*, 267, p. 1924, 1995.
- [BLY 79] BLYTHE A.R., *Electrical Properties of Polymers*, Cambridge University Press, 1979.
- [BOT 78] BOTTCHE C.J.F., BORDEWIJK P., *Theory of Electric Polarization*, vol. 2, Elsevier, Amsterdam, 1978.
- [BOY 75] BOYER R.F., *J. Polym. Sci. Symp.*, no. 50, 1, p. 182, 1975.
- [CAR 02] CARREGA M., *Les polymères: de la molécule à l'objet*, EDP Sciences, 1999.
- [COH 59] COHEN M.H., TURNBULL D., *J. Chem. Phys.*, 31, 5, p. 1164, 1959.
- [COL 41] COLE K.S., COLE R.H., *J. Chem. Phys.*, 9, 4, p. 341, 1941.
- [EYR 36] EYRING E., *J. Chem. Phys.*, 4, 4, p. 283, 1936.
- [FER 70] FERRY J.D., *Viscoelastic Properties of Polymers*, John Wiley, 1970.
- [FON 02] FONTANILLE M., GNANOU Y., *Chimie et physico-chimie des polymères*, Dunod, 2002.
- [FRO 58] FRÖLICH H., *Theory of Dielectrics*, Oxford University Press, 1958.
- [FUL 25] FULCHER G.S., *J. Am. Ceram. Soc.*, 8, 6, p.339, 1925.
- [HAL 06] HALARY J.L., LAUPRETRE F., *De la macromolécule au matériau polymère*, Belin, Paris, 2006.
- [HAV 97] HAVRILIAK S., HAVRILIAK S.J., *Dielectric and Spectroscopy of Polymeric Materials*, James P. Runt (ed.), American Chemical Society, Washington DC, 1997.
- [HAV 67] HAVRILIAK S., NAGAMI S., *Polymer*, 8, p. 161, 1967.
- [HED 77] HEDVIG P., *Dielectric Spectroscopy of Polymers*, A. Hilger Ltd, 1977.
- [HOF 66] HOFFMAN J.D., WILLIAMS G., PASSAGLIA E., *J. Polym. Science: Polym. Symp.*, 14, 1, p. 73, 1966.

- [JON 83] JONSCHER A.K., *Dielectric Relaxation in Solids*, Chelsea Dielectric Press, London, 1983.
- [KRE 02] KREMER F., SCHONHALS A., *Broad Band Dielectric Spectroscopy*, Springer, Berlin, 2002.
- [MCC 67] MC CRUM N.G., READ B.E., WILLIAMS G., *Anelastic and Dielectric Effects in Polymeric Solids*, Wiley, London, 1967.
- [MEN 99] MENEGOTTO J., Etude de la Mobilité Moléculaire dans les Polymères Linéaires à l'Etat Solide par Spectroscopies Diélectriques, Doctoral Thesis, University of Toulouse, 1999.
- [PER 92] PEREZ J., *Physique et mécanique des polymères amorphes*, Tech. et Doc, Lavoisier, 1992.
- [RAU 02] RAULT J., *Les polymères solides*, Cepadues, 2002.
- [RUN 97] RUNT J.P., FITZGERALD J.J., *Dielectric Spectroscopy of Polymeric Materials* ACS, 1997.
- [STA 81] STARKWEATHER H.W., *Macromolecules*, 14, 5, p. 1277, 1981.
- [STR 97] STROBL G., *The Physics of Polymers*, Springer, 1997.
- [STR 78] STRUIK L., *Physical aging in amorphous polymers and others materials*, Elsevier, 1978.
- [TAM 26] TAMMANN, Hesse G., *ANORG. Z., Allgem. Chem.*, 156, 1, p. 245, 1926.
- [VAN 75] VAN TURNHOUT J., *Thermally Stimulated Discharge of Polymer Electrets*, Elsevier, 1975.
- [VOG 21] VOGEL H., *Physik Zeitung*. 22, p. 645, 1921.